Electronic Supplementary Material (ESI) for Journal of Materials Chemistry

Supplementary Material for

Uniform PtIr catalysts Supported on Carbon Nanotube prpepared under assistance of PhosphomolybdicAcid, and their Enhanced Performance on the Oxidation of Methanol

Junhua Yuan[1*,2], Bo He[1], Liji Hong[1], Juan Lu[1], Jianguo Hu[1], Jigen Miao[1], Li Niu[3*]

[1]College of Life Sciences and Chemistry, Zhejiang Normal University, Jinhua, Zhejiang, 321004 (China)

[2] School of Pharmacy, Hubei University of Science and Technology

[3]State Key Laboratory of Electroanalytical Chemistry, Changchun Institute of Applied Chemistry, Chinese Academy of Sciences, Changchun, Jilin, 130022 (China)

[*]Corresponding author: Tel.:Fax:+86 579 82282269, E-mail address: jhyuan@zjnu.cn. (J Yuan), lniu@ciac.jl.cn (L. Niu)

Fig. S1

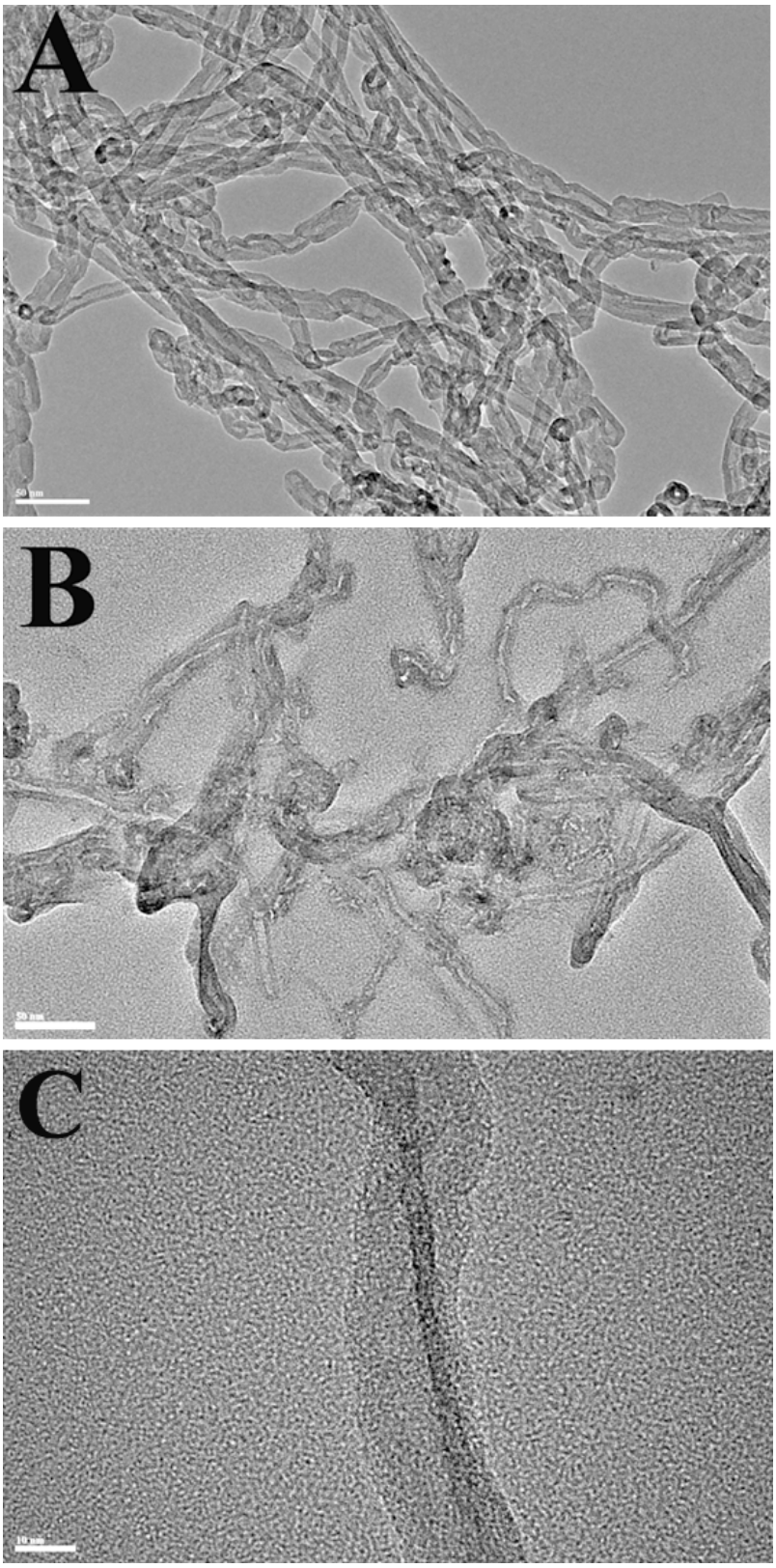

Fig. S1 TEM images of (A) MWCNTs and PMo/MWCNT hybrids in low magnification (B) and in high magnification (C).

Fig. S2

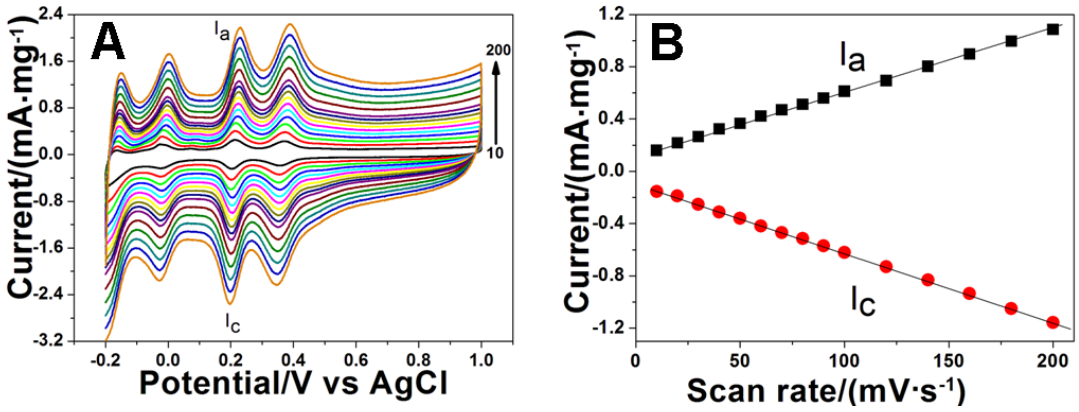

Fig. S2 The CV curves (A) of PMo/MWCNT hybrids at different scan rate in Nitrogen-saturated 0.5 M H_2SO_4 solution, and the corresponding dependence (B) of the peak (I) current on scan rate.

Fig. S3

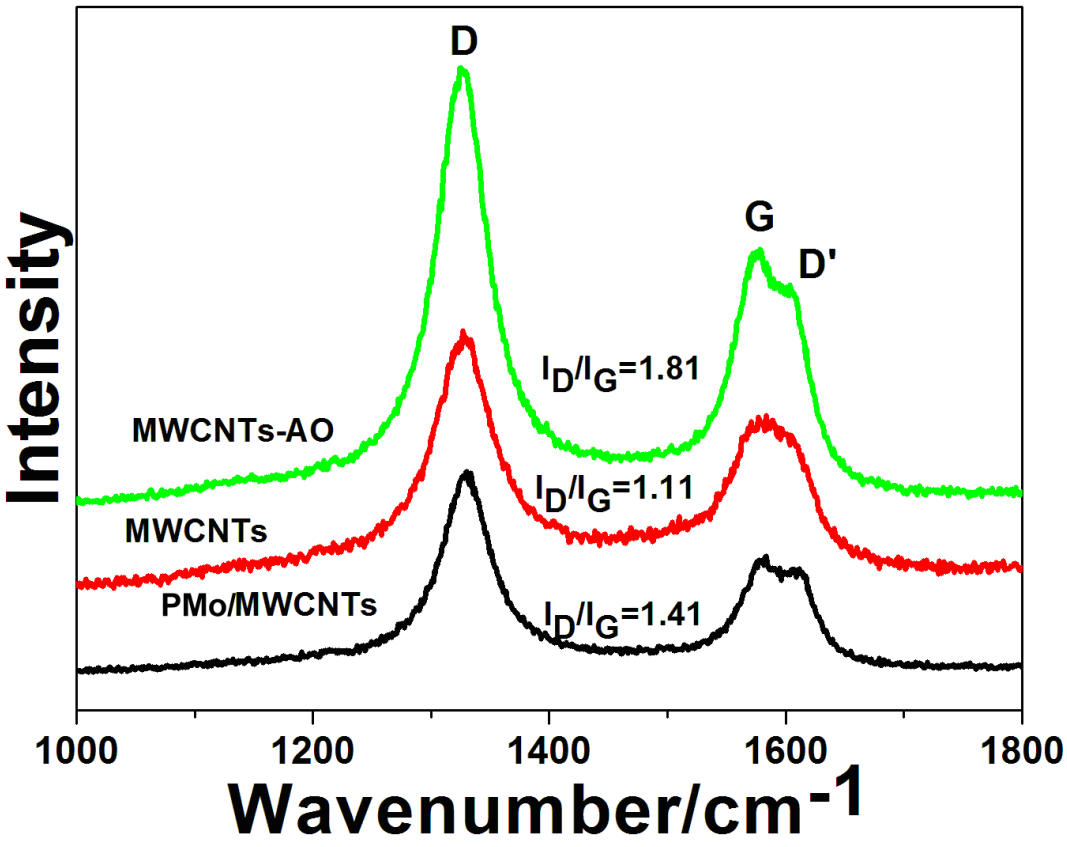

Fig. S3 The Raman spectra of the pristine PMo/MWCNTs, MWCNTs and MWCNTs-AO.

Fig. S3 shows the Raman spectra of the the pristine MWCNTs, PMo/MWCNT hybrids and acid-oxidized MWCNTs (MWCNTs-AO, refluxing MWCNTs in a mixed acid solution, H_2SO_4:HNO_3 in 1:3 v/v ratios, for 8 h.). In Figure S3, the peak at 1320 cm^{-1} should be assigned to the A_{1g} breathing mode of disorder graphite structure (i.e., the D band), and the peak at ~1570 cm^{-1} assigned to the E_{2g} structure mode of graphite (i.e., the G band). The G band reflects the structure of the sp2 hybridized

carbon atom. An additional side band at ~1600cm^{-1} was also observed, which was assigned as the D′ band. Both the D and the D′ bands are due to the defect sites in the hexagonal framework of graphite materials.[1] The extent of the defects in graphite materials can be quantified by the intensity ratio of the D to G bands (i.e., I_D/I_G). It can be obtained from Figure S3 that the values of the I_D/I_G ratio are 1.41, 1.11 and 1.81 for the pristine PMo/MWCNT hybrids, MWCNTs and MWCNTs-AO, respectively. The I_D/I_G value for the pristine CNTs (1.11) is in agreement with that reported in literature [2]. It is noted that the values of I_D/I_G ratio of both PMo/MWCNT hybrids and MWCNTs-AO are higher than that of the pristine CNTs due to the surface modification process. However, the CNTs-AO have higher I_D/I_G ratio than the PMo/MWCNTs, indicating that the harsh chemical acid treatment causes more structural damage of MWCNTs than the ultrosonic treatment CNT during the process of PMo modification. The results from Raman spectra in Figure S2 indicate that the PMo-modification process leads to the less structural damage of MWCNTs than the typical acid oxidized treatment, implying the PMo/MWCNTs should retain better electric conductivity than the CNTs-AO.

Fig. S4

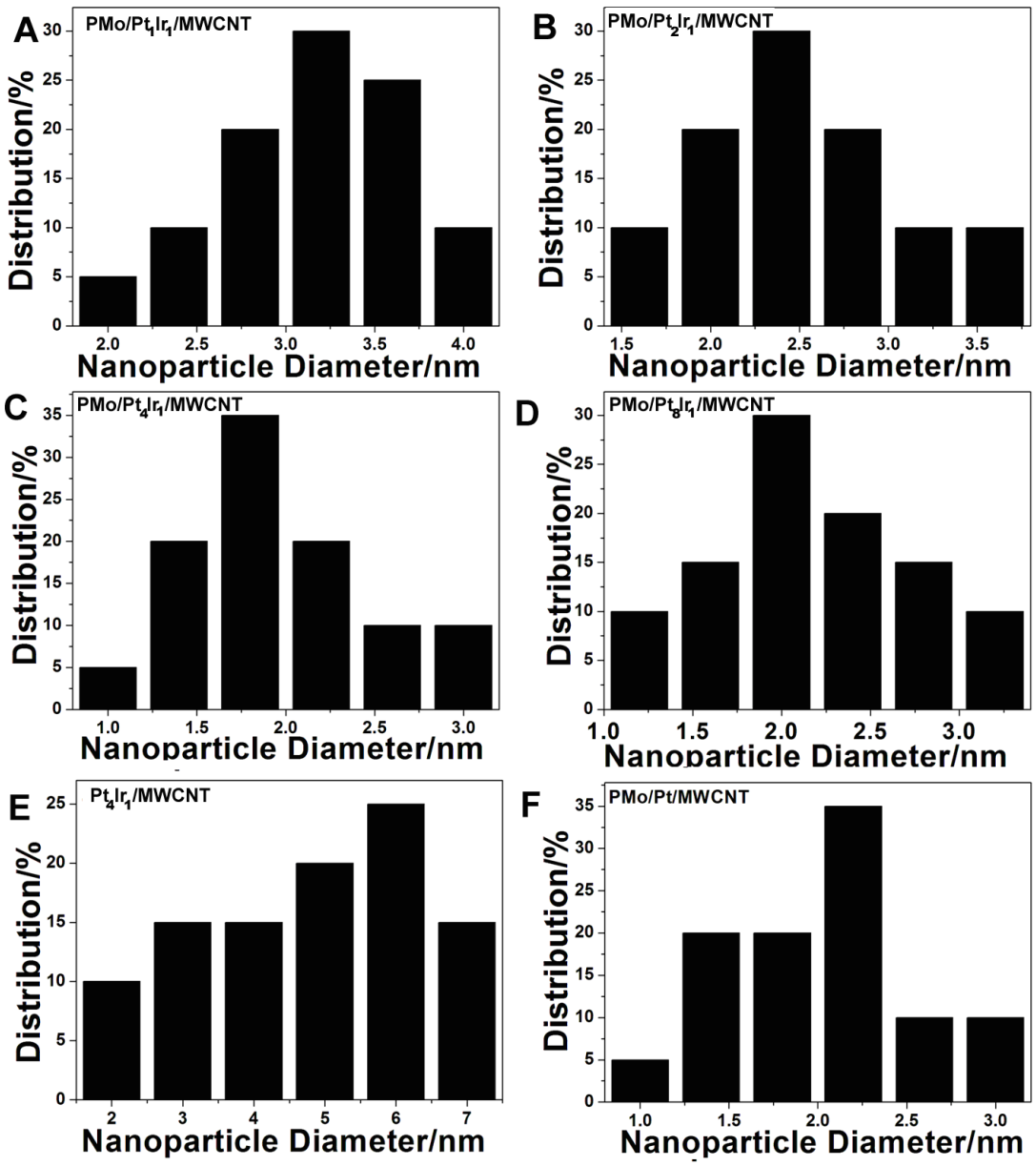

Fig. S4 Size distributions of PtIr (A, B, C, D and E), and Pt (F) nanoparticles in (A) PMo/Pt_1Ir_1/MWCNT, (B) PMo/Pt_2Ir_1/MWCNT, (C) PMo/Pt_4Ir_1/MWCNT, (D) PMo/Pt_8Ir_1/MWCNT, (E) Pt_4Ir_1/MWCNT and (F) PMo/Pt/MWCNT catalysts.

Table S1 The composition data of the different Pt and Pt alloy catalysts recorded by ICP-AES and EDS

Catalysts	Pt(wt%)[a]	Ir(wt%)[a]	Mo(wt%)[a]	Pt/Ir[b]
PMo/Pt_1Ir_1/MWCNT	9.16	9.10	2.12	1.01
PMo/Pt_2Ir_1/MWCNT	12.24	6.15	4.54	1.89
PMo/Pt_4Ir_1/MWCNT	14.66	3.64	5.70	3.91
PMo/Pt_8Ir_1/MWCNT	16.32	2.08	5.06	7.84
PMo/Pt/MWCNT	18.08	-	5.65	-
Pt_4Ir_1/MWCNT	14.59	3.82	-	3.82

a. These data come from ICP-AES

b. These data come from EDS

Fig. S5

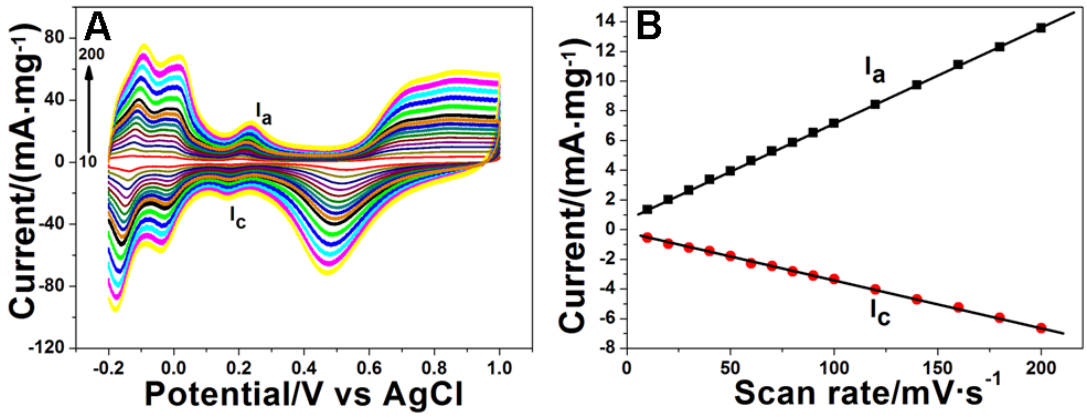

Fig. S5 The CV curves (A) of PMo/Pt_4Ir_1/MWCNT catalysts at different scan rate in Nitrogen-saturated 0.5 M H_2SO_4, solution, and the corresponding dependence (B) of the peak (I) current on scan rate.

Table S2 Pt loading ([Pt]), hydrogen adsorption charges ($Q_{H\text{-}ads}$), hydrogen desorption charges ($Q_{H\text{-}des}$) and ESA of different catalysts.

Catalysts	[Pt] ($\mu g \cdot cm^{-2}$)	$Q_{H\text{-}ads}$ ($mC \cdot cm^{-2}$)	$Q_{H\text{-}des}$ ($mC \cdot cm^{-2}$)	ESA [$m^2 \cdot g^{-1}$Pt]
PMo/Pt_1Ir_1/MWCNT	24.50	2.66	2.27	47.9
PMo/Pt_2Ir_1/MWCNT	28.06	4.08	3.25	62.0
PMo/Pt_4Ir_1/MWCNT	31.25	6.65	6.18	97.8
PMo/Pt_8Ir_1/MWCNT	34.72	6.02	5.36	78.0
PMo/Pt/MWCNT	33.04	3.86	3.58	53.6
Pt_4Ir_1/MWCNT	31.36	3.78	3.42	51.4

Table S3 The forward peak potential (E_f), backward peak potential (E_b), forward peak current (I_f) and backward peak current (I_b) of methanol electro-oxidation on the different catalysts.

Catalyst	I_f [mA·mg^{-1}]	E_f [mV]	I_b [mA·mg^{-1}]	E_b [mV]	I_f/I_b	I_f/ESA A·m^{-2}
PMo/Pt_1Ir_1/MWCNT	92	685	79	468	1.16	1.92
PMo/Pt_2Ir_1/MWCNT	138	714	116	497	1.19	2.22
PMo/Pt_4Ir_1/MWCNT	311	697	288	539	1.08	3.18
PMo/Pt_8Ir_1/MWCNT	183	697	183	497	1.00	2.35
PMo/Pt/MWCNT	121	738	178	521	0.68	2.26
Pt_4Ir_1/MWCNT	109	703	104	557	1.05	2.12

Reference

[1]Y. L. Hsin, K. C. Hwang, C. T. Yeh, *J. Am. Chem. Soc.* **2007**, 129, 9999-10010.

[2] S.Y. Wang, X. Wang, S.P. Jiang, *Langmuir* **2008**, 24, 10505-10512.